1521-009X/42/4/511–519$25.00
Drug Metabolism and Disposition
http://dx.doi.org/10.1124/dmd.113.055418
Drug Metab Dispos 42:511–519, April 2014

N-Oxide Reduction of Quinoxaline-1,4-Dioxides Catalyzed by Porcine Aldehyde Oxidase SsAOX1[S]

Peiqiang Mu, Ming Zheng, Ming Xu, Yuanming Zheng, Xianqing Tang, Yufan Wang, Kaixin Wu, Qingmei Chen, Lijuan Wang, and Yiqun Deng

Guangdong Provincial Key Laboratory of Protein Function and Regulation in Agricultural Organisms, College of Life Sciences, South China Agricultural University, Guangzhou, Guangdong, China

Received October 13, 2013; accepted January 17, 2014

ABSTRACT

Quinoxaline-1,4-dioxides (QdNOs) are a class of quinoxaline derivatives that are widely used in humans or animals as drugs or feed additives. However, the metabolic mechanism, especially the involved enzymes, has not been reported in detail. In this study, the *N*-oxide reduction enzyme, porcine aldehyde oxidase SsAOX1 was identified and characterized. The *SsAOX1* gene was cloned from pig liver through reverse-transcription polymerase chain reaction using degenerate primers, which encode a 147-kDa protein with typical aldehyde oxidase motifs, two [2Fe-2S] centers, a flavin adenine dinucleotide (FAD) binding domain, and a molybdenum cofactor domain. After heterologous expression in a prokaryote, purified SsAOX1 formed a functional homodimer under native conditions. Importantly, the SsAOX1 catalyzed the *N*-oxide reduction at the N1 position of three representative QdNOs (quinocetone, mequindox, and cyadox), which are commonly used as animal feed additives. SsAOX1 has the highest activity toward quinocetone, followed by mequindox and cyadox, with $k$cat/K_m values of 1.94 ± 0.04, 1.27 ± 0.15, and 0.43 ± 0.09 minute^{-1} μM^{-1}, respectively. However, SsAOX1 has the lowest substrate affinity for quinocetone, followed by the cyadox and mequindox, with K_m values of 4.36 ± 0.56, 3.16 ± 0.48, and 2.96 ± 0.51 μM, respectively. In addition, using site-directed mutagenesis, we found that substitution of glycine 1019 with threonine endows SsAOX1 with *N*-oxide reductive activity at the N4 position. The goal of this study was to identify and characterize the *N*-oxide reduction enzyme for a class of veterinary drugs, QdNOs, which will aid in the elucidation of the metabolic pathways of QdNOs and will provide a theoretical basis for their administration and new veterinary drug design.

Introduction

The quinoxaline-1,4-di-*N*-oxides (QdNOs) are a class of quinoxaline derivatives that possess two N-O bonds at positions N1 and N4, respectively. QdNOs have a wide range of biologic properties, such as antibacterial, antiviral, antifungal, antiprotozoal, and anticancer activities (Carta et al., 2005), and have been widely used as human drugs or animal feed additives since the 1940s (Vicente et al., 2011).

The *N*-oxide groups are considered to be the main functional moiety of QdNOs. The presence of *N*-oxide groups in the molecular structures of the QdNOs leads to their antibacterial, antifungal, or antitumor effects in humans and animals (Carta et al., 2005). The presence of *N*-oxide groups in the quinoxaline ring has been shown to be necessary for the antitubercular activity of 3-chloro-2-quinoxalinecarbonitrile (Ortega et al., 2001). The *N*-oxide-reduced products of quindoxin have been shown to lose nearly all of the antibacterial activity (Suter et al., 1978). However, the *N*-oxide groups have also been shown to result in the toxicity of QdNOs. The mutagenic potency of QdNOs depends on the number of N-O bonds in their structure, because the reduced derivative of quindoxin, quinoxaline, was not mutagenic, and the partially reduced derivative, quinoxaline 1-oxide, exhibited lower mutagenic activity than quindoxin (Beutin et al., 1981). The *N*-oxide-reduced product of mequindox, quinoxaline-2-carboxylice acid, did not cause cell death, whereas mequindox produced significant reactive oxygen species and caused cell death to porcine adrenocortical cells (Huang et al., 2010).

Because of the vital roles of *N*-oxide groups in their activity and toxicity, the elucidation of the metabolic mechanism of the *N*-oxide groups in QdNOs is helpful for their administration and new veterinary drug design. Numerous reports have showed that the *N*-oxide groups can be reduced back to their parent amines (Bickel, 1969; Kitamura et al., 1999; Takekawa et al., 2001; Liu et al., 2010a,b; Liu and Sun, 2013). Cyadox was has been shown to be metabolized primarily into *N*-oxide-reduced products in rat, chicken, and swine (Beedham, 1987; Takekawa et al., 1997; Garattini et al., 2008; Zheng et al., 2011). The *N*-oxide reduction was also one of the main metabolic pathways of quinocetone in swine (Wu et al., 2012), and the N1-reduced quinocetone, 1-deoxyquinocetone, was significantly more abundant than other metabolites in swine urine (Shen et al., 2010). A similar phenomenon was also observed with mequindox. The 1-deoxymequindox, which is the N1-reduced mequindox, has been reported to be significantly higher than N4-reduced mequindox and other metabolites

This work was supported by the National Basic Research Program of China (973 Program) [Grant 2009CB118802], the National Natural Science Foundation of China [Grant 31172087], and the Specialized Research Fund for the Doctoral Program of Higher Education of China [Grant 20114404110010].

P.M. and M.Z. contributed equally to this work.

dx.doi.org/10.1124/dmd.113.055418.

[S] This article has supplemental material available at dmd.aspetjournals.org.

ABBREVIATIONS: AO, aldehyde oxidase; CD, circular dichroism; dNTP, deoxynucleotide triphosphate; FAD, flavin adenine dinucleotide; HPLC, high-performance liquid chromatography; KOD, *Thermococcus kodakaraensis*; LB, Luria-Bertani; PCR, polymerase chain reaction; TBST, Tris-buffered saline/Tween 20; QdNO, quinoxaline-1,4-dioxide; XO, xanthine oxidoreductase.

in chicken (Shan et al., 2012). Although it was widely reported that *N*-oxide reduction is the main metabolic pathway of QdNOs, the responsible enzyme, especially the specific isoforms of the enzyme, has been rarely reported. The liver has been found to play the dominant role in this reductive transformation. Several enzymes in the liver have been shown to be capable of catalyzing the *N*-oxide reduction. Brucine *N*-oxide can be reduced back to its parent tertiary amine by aldehyde oxidase (AO) (Takekawa et al., 1997, 2001; Kitamura et al., 1999). Using an enzyme inhibition approach, we demonstrated previously that the *N*-oxide reduction of cyadox might be catalyzed by AO and xanthine oxidoreductase (XO) (Zheng et al., 2011). Thus, it is interesting to examine whether AO has a function in the *N*-oxide reduction of QdNOs.

AOs (EC 1.2.3.1) are a small group of structurally conserved proteins belonging to the large family of molybdo-flavoenzymes, which play important physiologic and pharmacologic roles in various plants and animals (Beedham, 1987; Hille, 1996; Garattini et al., 2008). AO is composed of two homogenous monomers, with each subunit having a molecular mass of approximately 150 kDa (Hille, 2005). Each subunit contains two nonidentical 2Fe–2S redox centers in the *N*-terminus, a FAD-binding domain at the center, and a substrate-binding pocket in close proximity to the molybdenum cofactor in the C terminus (Pryde et al., 2010; Garattini and Terao, 2013). AO is capable of oxidizing numerous aldehydes, such as benzaldehyde and 2-hydroxyprimidine, and a variety of *N*-heterocyclic compounds in the presence of an electron donor, such as sulfoxides and azo dyes (Hille, 2002; Garattini et al., 2008). Many cDNAs coding for AO from various species have been cloned. Pigs, which are an important food source of humans, are exposed to significant amounts of drugs and toxins, including QdNOs as a feed additive. However, the AO for QdNOs has not been identified and reported.

In this study, a gene encoding AO from pig liver has been cloned and tested for its ability to catalyze the *N*-oxide reduction of three widely used QdNOs (quinocetone, mequindox, and cyadox) (Fig. 1), and the catalytic mechanism was analyzed by site-directed mutagenesis.

Materials and Methods

Chemicals and Reagents. Quinocetone ($C_{18}H_{14}N_2O_3$, 99.8%), 1-deoxyquinocetone ($C_{18}H_{14}N_2O_2$, 99.8%), 4-deoxyquinocetone ($C_{18}H_{14}N_2O_2$, 99.8%), 1,4-dideoxyquinocetone ($C_{18}H_{14}N_2O$, 99.8%), mequindox ($C_{11}H_{10}N_2O_3$, 99.8%), 1-deoxymequindox ($C_{11}H_{10}N_2O_2$, 99.8%), 4-deoxymequindox ($C_{11}H_{10}N_2O_2$, 99.8%), 1,4-dideoxymequindox ($C_{11}H_{10}N_2O$, 99.8%), cyadox ($C_{12}H_9N_5O_3$, 99.8%), 1-deoxycyadox ($C_{12}H_9N_5O_2$, 99.8%), 4-deoxycyadox ($C_{12}H_9N_5O_2$, 99.8%), and 1,4-dideoxycyadox ($C_{12}H_9N_5$, 99.8%) were synthesized at the Institute of Veterinary Pharmaceuticals (Wuhan, China). The high-performance liquid chromatography

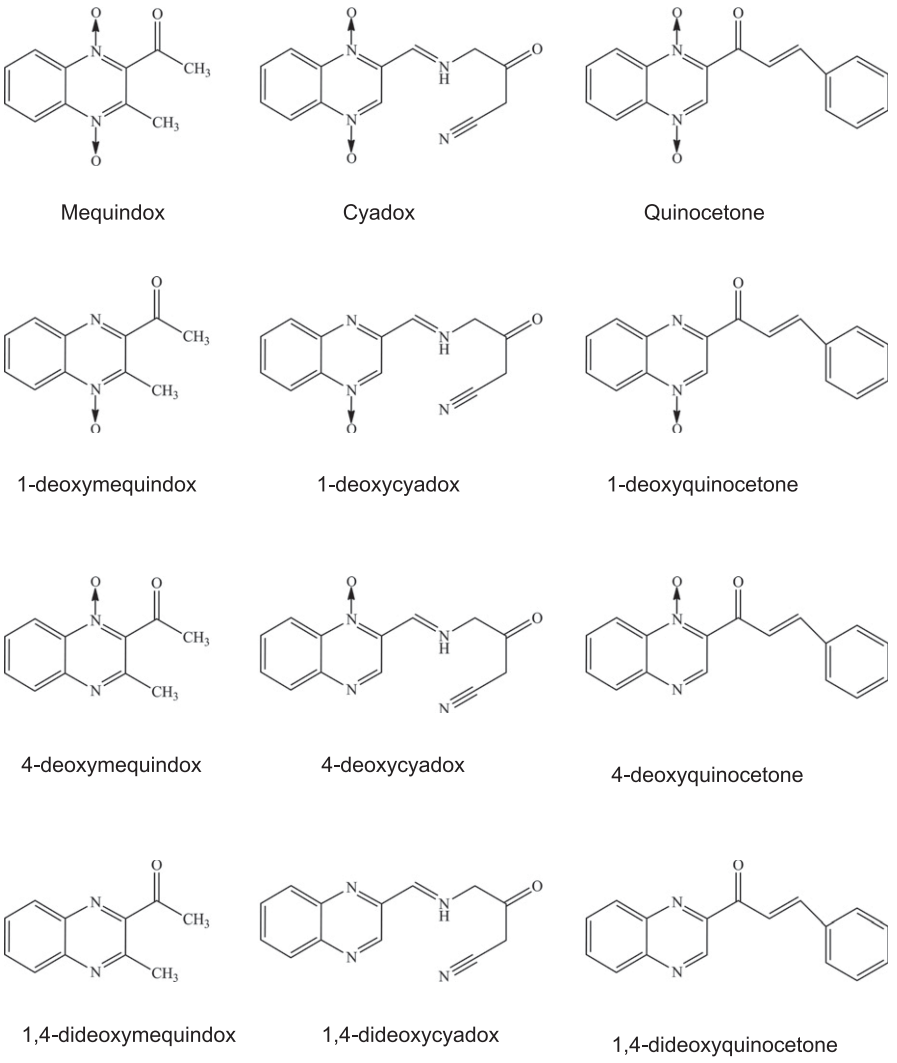

Fig. 1. Molecular structures of the quinoxaline 1,4-di-*N*-oxides used in this study.

(HPLC) graphs for these entities are shown in Supplemental Figs. 1–3. Benzaldehyde was purchased from the Sigma-Aldrich Company (St. Louis, MO). HPLC-grade methanol was purchased from Thermo Fisher Scientific (Fairlawn, NJ). Ultrapurified water was obtained from a Milli-Q ultrapurification system (Millipore, Bedford, MA). The restriction enzymes were purchased from Takara (Dalian, China). All of the other chemicals and reagents commercially available were of the highest analytical grade.

Animals. The animal studies were approved by the Institutional Animal Care and Use Committee of South China Agricultural University, and adhered to the Chinese Guidelines for the Proper Conduct of Animal Experiments for the use of laboratory animals. Five-month-old female Danish Landrace × Yorkshire × Duroc cross-bred pigs were purchased from the College of Veterinary Medicine at the South China Agricultural University. The pigs were fed standard commercial diets and had access to water ad libitum before being sacrificed. Immediately after the pigs were sacrificed by bleeding from the carotid artery, the liver was isolated and frozen in liquid nitrogen.

cDNA Cloning of Aldehyde Oxidase from Pig Liver. Total RNA from pig liver was extracted using the SV Total RNA Isolation System (Promega, Madison, WI) according to the manufacturer's instructions. To obtain total cDNA for gene amplification, random primers were used to perform reverse-transcription polymerase chain reaction (PCR) using first-strand cDNA, which was synthesized using the SMART MMLV Reverse Transcriptase (Clontech, Mountain view, CA). Based on the available sequenced genome of *Sus scrofa*, four AO genes originating from *Mus musculus* were used as probes to screen the corresponding homologs. Considering the specificity and degeneracy, the alignment of the four AOX1s originating from human, cow, mouse, and rat samples was performed. Three pairs of degenerate primers were designed by Genefisher2 (http://bibiserv.techfak.uni-bielefeld.de/genefisher2). The primer sequences are listed in Supplemental Table 1. PCR was conducted in a 50 μl solution containing *Thermococcus kodakaraensis* (KOD) FX buffer, 200 mM deoxynucleotide triphosphate (dNTP) solution, 2 U of KOD FX DNA polymerase (Toyobo, Osaka, Japan), 2 mM $MgCl_2$, 1 mM of each primer, and 1 μl of total cDNA as a template. PCR amplifications were conducted as follows: initial denaturation at 94°C for 2 minutes, 35 cycles of 94°C for 30 seconds, 55°C for 30 seconds, 68°C for 2 minutes, and a final extension at 68°C for 10 minutes. The PCR products were cloned into the pMD20-T vector (TaKaRa, Qingdao, China) and verified by sequencing. All three sequences of the AO fragment contained an overlapping region for assembling the full-length sequence of the porcine AO. The deduced full-length sequence was used to derive the unique primers for the porcine AO. The forward and reverse primers were 5'-ATGGACGGGGCGGCGGAGCTG-3' and 5'-TCATATGGGTACACTC-CAAGG-3', respectively. The reaction was conducted in a 50-ml solution containing KOD-plus buffer, 200 mM dNTP solution, 2 U of KOD-plus polymerase (Toyobo), 2 mM $MgCl_2$, 1 mM of each primer, and 1 μl of the template. PCR amplifications were performed as follows: initial denaturation at 94°C for 2 minutes, 35 cycles of 94°C for 30 seconds, 60°C for 30 seconds, 68°C for 4 minutes, and a final extension at 68°C for 5 minutes. The PCR product was cloned into the pMD20-T vector and sequenced.

Bioinformatics and Statistical Analysis. The BLAST algorithm (http://blast.ncbi.nlm.nih.gov/) was used to retrieve nucleotide sequences highly similar to the porcine AOX 1 gene (GenBank accession no. JX977168). The exon-intron junctions were analyzed with an Internet splice program (http://www.fruitfly.org/seq_tools/splice.html). The amino acid sequence analysis was performed using the EMBOSS Transeq program for publication (http://www.ebi.ac.uk/Tools/st/emboss_transeq). Motif prediction was performed by the National Center for Biotechnology Information's conserved domain search (http://www.ncbi.nlm.nih.gov/Structure/cdd/wrpsb.cgi). Sequence alignments were performed using the ClustalW algorithms (http://www.ebi.ac.uk/Tools/msa/clustalw2). Statistical analyses were performed using the GraphPad Prism program, version 5.0 for Windows XP.

Construction of the SsAOX1 Expression Vector. The obtained cDNA was used as a template for the synthesis of PCR fragments with an expected size of 4,017 bp. The primers used for amplification were 5′-CAAGCTTCTATG-GACGGGGCGGCGGAG-3′ (forward), with an introduced HindIII restriction site, and 5′-ATAAGAATGCGGCCGC TCATATGGGTACACTCCAAG-3′ (reverse), with an introduced NotI restriction site. The reaction was conducted in a 50 ml solution containing KOD-plus buffer, 200 mM dNTP solution, 2 U of KOD-plus polymerase (Toyobo), 2 mM $MgCl_2$, 1 mM of each primer, and 1 μl of the template. PCR amplifications were conducted as follows: initial denaturation at 94°C for 2 minutes, 35 cycles of 94°C for 30 seconds, 60°C for 30 seconds, 68°C for 4 minutes, and a final extension at 68°C for 5 minutes. The amplified DNA (20 mg) was cleaved with HindIII and NotI (New England BioLabs, Beverly, MA). The resulting DNA fragment was cloned into the pQE-30 Xa vector (20 mg; QIAGEN, Venlo, The Netherlands) using the TaKaRa DNA Ligation Kit Ver. 2 (TaKaRa) according to the manufacturer's protocol. Subsequently, 5 μl of the diluted ligation reaction was transformed into 50 μl of DH5α-competent cells. The transformants were plated on Luria-Bertani (LB) agar plates containing 100 μg/ml ampicillin and grown overnight at 37°C. Plasmid DNA from several colonies was isolated using a TIANGEN Spin Miniprep Kit (TIANGEN), and screened by restriction digestion with HindIII and NotI. A positive colony was replated and grown overnight at 37°C. A single colony was then selected and grown overnight in LB broth containing 100 μg/ml ampicillin, and the plasmid DNA was isolated and verified by sequencing.

Prokaryotic Expression and Purification of Recombinant SsAOX1. The pQE-30 plasmid containing the *SsAOX1* cDNA was transformed into M15-competent cells and grown on LB agarose plates containing 100 μg/ml ampicillin. A single colony was selected and grown overnight in 100 ml of supplemented LB broth (100 μg/ml ampicillin, 1 μg/ml riboflavin, and 50 μM sodium molybdate). The overnight culture (10 ml) was used to inoculate 500 ml of supplemented Terrific broth (100 μg/ml ampicillin, 250 μl of trace element solution containing 2.7 g of $FeCl_3 \cdot 6H_2O$, 0.2 g of $ZnCl_2 \cdot 4H_2O$, 0.2 g of $CoCl_2 \cdot 6H_2O$, 0.2 g $Na_2MoO_4 \cdot 2H_2O$, 0.2 g of $CaCl_2 \cdot H_2O$, 0.1 g of $CuCl_2$, 0.05 g of H_3BO_3, and 10 ml of concentrated HCl autoclaved in a total volume of 100 ml of double-distilled H_2O, 1 μg/ml riboflavin, and an additional 50 μM sodium molybdate). Cultures were grown at 37°C and 250 rpm until an absorbance of 0.4 at 600 nm was reached for 60 to 90 minutes; the addition of 1 mM IPTG was performed for induction, and the cells were allowed to continue growing at room temperature for 72 hours at 150 rpm. The cells were chilled on ice and harvested by centrifugation at 3500*g* at 4°C for 30 minutes. The cell pellet was resuspended in 100 mM Tris acetate buffer (pH 7.6) containing 500 mM sucrose and 0.5 mM EDTA, and diluted with an equal volume of ice-cold water. Lysozyme was then added to the resuspended cells to a final concentration of 0.25 mg/ml. The suspension was placed on a shaker at 4°C for 45 minutes. The spheroplasts were pelleted at 2800*g* for 20 minutes at 4°C and resuspended in 100 mM potassium phosphate buffer (pH 7.6) containing 6 mM magnesium acetate, 20% glycerol (v/v), and 0.1 mM dithiothreitol. The suspensions were sonicated on ice and centrifuged at 75,000*g* for 20 minutes at 4°C. The 6×His-tagged proteins were purified using nickel-nitrilotriacetic acid (Ni-NTA) affinity chromatography. The AO proteins were eluted in buffer containing 50 mM potassium phosphate (pH 7.4), 300 mM NaCl, and 500 mM imidazole. Proteins were extensively dialyzed for 12 hours in 50 mM potassium phosphate buffer containing 10% glycerine at 4°C, with two buffer changes. After dialysis, the proteins were aliquoted and stored at −80°C until use. The protein concentrations were determined by the Bradford assay using bovine serum albumin as a standard.

Western Blot Analysis. Protein samples from the induced bacteria were separated on 7.5% SDS-PAGE gels and then electrophoretically transferred to a polyvinylidene difluoride membrane (PALL, Ann Arbor, MI). The membrane was blocked with freshly prepared Tris-buffered saline/Tween 20 (TBST) buffer (25 mM of Tris-HCl [pH 7.5], 150 mM of NaCl, and 0.1% Tween-20) containing 5% nonfat dry milk for 1 hour at room temperature and incubated for 1 hour with a rabbit polyclonal antibody against AOX1 (1:1000 dilution; sc-98500; Santa Cruz Biotechnology, Santa Cruz, CA) in TBST buffer containing 1% milk. After three 10-minute washes with TBST, the membranes were incubated with an HRP-rabbit anti-mouse IgG (γ) (Invitrogen, Carlsbad, CA) at 1:4000 for 1 hour at room temperature and then washed for another 30 minutes with TBST buffer. Band detection was performed using the LumiGLO Chemiluminescent Substrate Kit (CST, Beverly, MA), according to the manufacturer's instructions. Chemiluminescence was quantified using the Quantity Tools of Image Laboratory software (Bio-Rad, Hercules, CA).

Circular Dichroism Spectroscopy. Wide-type AO was tested at 5 μM in 100 mM potassium phosphate buffer (pH 7.4). The circular dichroism (CD) spectra of these samples were obtained on a Chirascan apparatus (Applied Photophysics Limited, Leatherhead, Surrey, UK) at 25°C using a bandwidth of 1 nm, a cell path length of 1 mm, a step of 1.0 nm, a time-per-point of

0.5 second, and a time interval of 1.0 minute. The value for the buffer alone was measured and subtracted from the protein spectra. All of the spectra were collected using a protein concentration of 0.05 mg/ml. The data were converted and normalized to the molar ellipticity ([θ]), in degrees·cm^2·dmol^{-1}.

Native PAGE. The purified SsAOX1 in native PAGE sample buffer (50 mM Tris-HCl (pH 6.8), 10% glycerol, and 0.01% bromophenol blue) and boiled SsAOX1 in denatured buffer (50 mM Tris-HCl [pH 6.8], 1% SDS, 1% β-mercaptoethanol, 10% glycerol, and 0.01% bromophenol blue) was separated

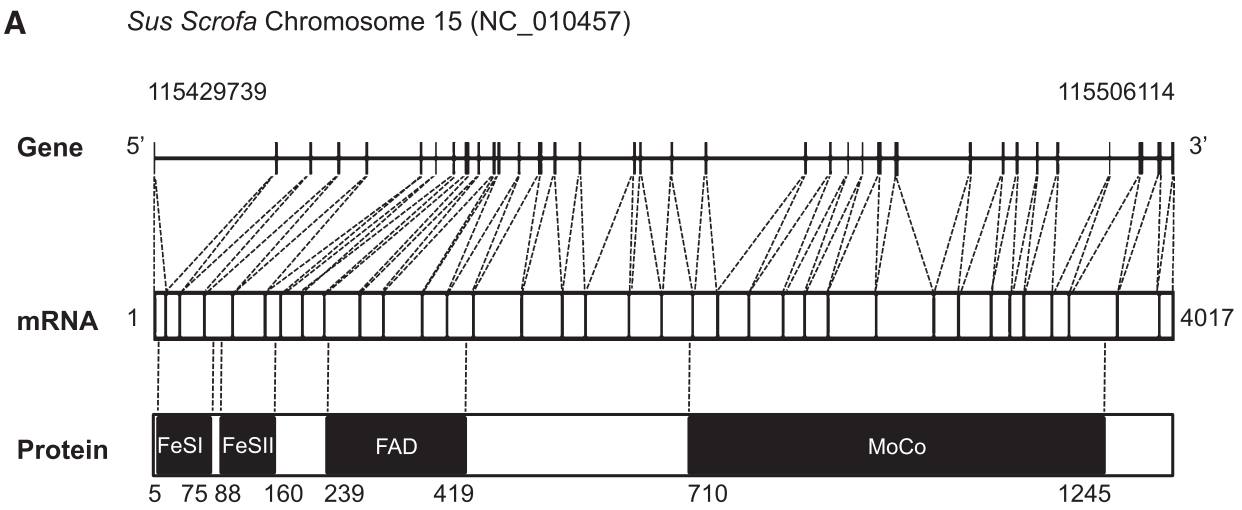

B

```
                                                    FeSI
SsAOX1 5   AELLFYVNGRKVIEKNVNPETMLLPYLRKKLRLTGTKYGCGGGGCGACTVMISRYNPITKRIRHYPANACL75..88TVEGIGSTRTRIHPVQERIAK 108
BtAOX1 5   SELLFYVNGRKVTEKNVDPETMLLPYLRKKLRLTGTKYGCGGGGCGACTVMISRYNPITKKIRHYPANACL75..88TVEGIGSTKTRIHPVQERIAK 108
HsAOX1 5   SELLFYVNGRKVIEKNVDPETMLLPYLRKKLRLTGTKYGCGGGGCGACTVMISRYNPITKRIRHHPANACL75..88TVEGIGSTHTRIHPVQERIAK 108
MmAOX1 5   SELLFYVNGRKVIEKNVDPETMLLPYLRKKLRLTGTKYGCGGGGCGACTVMISRYNPITKRIRHHPANACL75..88TVEGIGSTHTRIHPVQERIAK 108
PaAOX1 5   PELLFYVNGRKVVEKQVDPETMLLPYLRKKLRLTGTKYGCGGGGCGACTVMISRYNRVTKKIRHYPVNACL75..88TVEGIGSTTTRLHPVQERIAK 108
OcAOX1 5   IQLLFYVNGQKVVEKNVDPEMMLLPYLRKNLRLTGTKYGCGGGGCGACTVMISRYNPSTKAIRHHPVNACL74..87TVEGLGNTRTRLHPIQERIAK 107
RnAOX1 4   PQLLFYVNGQKVVENNVDPEMMLLPYLRKNLRLTGTKYGCGGGGCGACTVMISRYNPSTKSIRHHPVNACL74..87TVEGIGNTRTRLHPVQERIAK 107
           :*******:** *::*:** ********:*************************  ** ***:*.****      ****:*.* **:**:*******

                                                    FeSII
SsAOX1 109 CHGTQCGFCTPGMVMSIYTLLRNHPEPTLSQLTEALGGNLCRCTGYRPITDA160..239FGGDRMTWISPVTLKELLEAKVKYPQAPVVMGNTSVGP 273
BtAOX1 109 CHGTQCGFCTPGMVMSLYTLLRNHPEPTLTQLNDALGGNLCRCTGYRPIINA160..239FGSDRMTWISPVTLKELLEAKVKYPQAPVVMGNTSVGP 273
HsAOX1 109 CHGTQCGFCTPGMVMSIYTLLRNHPEPTLDQLTDALGGNLCRCTGYRPIIDA160..239FGSERMMWFSPVTLKELLEFKFKYPQAPVIMGNTSVGP 273
MmAOX1 109 CHGTQCGFCTPGMVMSIYTLLRNHPEPTLDQLTDALGGNLCRCTGYRPIIDA160..239FSGERMMWFSPVTLKELLEFKFKYPQAPVVMGNTSVGP 273
PaAOX1 109 FHGTQCGFCTPGMVMSMYALLRNHPEPTLDQLADALGGNLCRCTGYRPIIEA160..239FSGERMMWISPVTLKALLEAKSTYPQAPVVMGNTSVGP 273
OcAOX1 108 CHGTQCGFCTPGMVMSMYALLRNHPEPTLDQLTDALGGNLCRCTGYRPIIDA159..238FYGERVTWISPVTLKELVEAKFKYPQAPIVMGYTSVGP 272
RnAOX1 108 CHSTQCGFCTPARVMSMYALLRNHPEPSLDQLTDALGGNLCRCTGYRPIIDA159..238FYSNRMTWISPVTLEELVEAKFKYPGAPIVMGYTSVGP 272
           .*.********. ***:*:********:* ** :*****************:*       * .:*: *:*****: *:* * .** **::** *****

                                                    FAD
SsAOX1 274 DVKFKGIFHPVIISPDSIPEMSIVNYTDNGLTLGAALSLAQVKDILAKVLRKLPEEKTQTFHALWKHLGTLAGAQIENMSSIGGHLVSRHLDSDLNPL 371
BtAOX1 274 DMKFKGIFHPVIISPDRIEELSVVNYTDNGLTLGAAVSLAEVKDILANVTRKLPEEKTQMYHALLKHLETLAGPQIRNMASLGGHIVSRHPDSDLNPL 371
HsAOX1 274 EVKFKGVFHPVIISPDRIEELSVVNHAYNGLTLGAGLSLAQVKDILADVVQKLPEEKTQMYHALLKHLGTLAGSQIRNMASLGGHIISRHPDSDLNPI 371
MmAOX1 274 EVKFKGVFHPVIISPDRIEELSVVNHAYNGLTLGAGLSLAQVKDILADVVQKLPEEKTQMYHALLKHLGTLAGSQIRNMASLGGHIISRHPDSDLNPI 371
PaAOX1 274 GVKFKGIFHPVIISPDSIEELNVVSHTHSGLTLGAGLSLAQVKDILADVVQKVPEENAQTYRALLKHLGTLAGSQIRNMASLGGHIISRHLDSDLNPL 371
OcAOX1 273 EVKFKGVFHPIIISPDRIEELGVISQARDGLTLGAGLSLDQVKDILADIVQKLPEEKTQTYRALLKHLRTLAGSQIRNMASLGGHIVSRHLDSDLNPL 371
RnAOX1 273 EVKFKGVFHPIIISPDRIEELSIINQTGDGLTLGAGLSLDQVKDILTDVVQKLPEETTQTYRALLKHLRTLAGSQIRNMASLGGHIVSRHLDSDLNPL 370
           :****:***::**** ***:.::. :  .******.:** :*****:.: :*:***.:* ::** *** ****.*****:******:*** ******: 370

SsAOX1 371 LAVGNCTLNLQSKEGKRQIPLNFQFLKKCPSASLKPEPILISVNIPYS419..710EAIQHKSFFEQEKKLEYGNVDEAFKMVDQVLEGEIHLGGQEH 750
BtAOX1 371 LAVGNCTLNLLSKEGRRQIPLNEQFLRKCPSADLKPEEILISVNIPYS419..709EAIQNKSFFEPERKLEYGNVDEAFKMVDQILEGEIHMGGQEH 750
HsAOX1 371 LAVGNCTLNLLSKEGKRQIPLNEQFLSKCPNADLKPQEILVSVNIPYS419..710ESIQHNSSFKPERKLEYGNVDEAFKVVDQILEGEIHMGGQEH 750
MmAOX1 371 LAVGNCTLNLLSKEGKRQIPLNEQFLSKCPNADLKPQEILVSVNIPYS419..710ESIQHNSFFEPERKLEYGNVDEAFKVVDQILEGEIHMGGQEH 750
PaAOX  371 LAVGNCTLNVLSKEGERQIPLDEQFLSRCPEADLKPQEILASVHIPYS418..706EAIEQKSFFEPERKLEYGNVDEAFKVVDQILEGEIHMGGQEH 750
OcAOX  370 LAVGNCTLNLLSKDGERRIPLSEEFLRKCPEADLKPQEVLVSVNIPWS419..705EAIQHKSFFKSERKLECGNVDEAFKIVDQILEGEIHIGGQEH 750
RnAOX1 370 LAVGNCTLNLLSKDGKRQIPLSEQFLRKCPDSDLKPQEVLVSVNIPCS418..705EAIQHKSFFESERKLECGNVDEAFKIADQILEGEIHIGGQEH 750
           *********: **:*.*:***.*:** :**.:.***:*:* **:** *       *:*:::* *: *:*** ********:.**:******:*****

                                                    MoCo
SsAOX1 1000..NYWKKKGLAVVPLKYPVGTGSLAMGQAAALVHIYLDGSVLVTHGGIEMGQGVHTKMLQVASRELRMPLSNIHLRGTSTETIPNANISGGSVVAD.. 1093
BtAOX1 1001..NYWKKKGLAMVPLKYPIGLGSVAAGQAAALVHIYLDGSVLVTHGGIEMGQGVHTKMIQVVSRELRMPLSSIHLRGTSTETIPNTNPSGGSVVAD.. 1094
HsAOX1 1000..NYWKKKGLAMVPLKFPVGLGSRAAGQAAALVHIYLDGSVLVTHGGIEMGQGVHTKMIQVVSRELRMPMSNVHLRGTSTETVPNANISGGSVVAD.. 1091
MmAOX1 1000..NYWKKKGLAMVPLKYPVGLGSRAAGQAAALVHIYLDGSVLVTHGGIEMGQGVHTKMIQVVSRELRMPMSNVHLRGTSTETVPNANISGGSVVAD.. 1093
PaAOX1 996 ..NYWKQRGLAIIPFKYPRGLGSVAYGQAAALVHVYLDGSVLVTHGGIEMGQGVHTKMIQVVSRELKMPMSNVHLRGTSTETVPNTNASGGSVVAD.. 1089
OcAOX1 995 ..NSWKKRGMAVIPLKFPVGIGSVAMGQAAALVHIYLDGSALVSHGGIEMGQGVHTKMIQVVSRELRMPMSSVHLRGTSTETVPNTNASGGSVVAD.. 1088
RnAOX1 995 ..NSWKKRGMAVIPLKFPVGVGSVAMGQAAALVHIYLDGSALVSHGGIEMGQGVHTKMIQVVSRELKMPMSSVHLRGTSTETVPNTNASGGSVVAD.. 1088
             * **::*:*::*:*:* * ** * ********:******.**:***************:**.****:**:*.:*********:**:* ********
```

Fig. 2. The gene exon-intron structure, predicted motifs of SsAOX1, and their conservation among mammalian AOX1s. (A) The location of exon-intron structures of *SsAOX1* and the predicted motifs of its deduced amino acid sequences. (B) The alignment of SsAOX1 with other mammalian AOX1s. Identical amino acids among all of the aligned sequences are marked with an asterisk, and the conserved amino acids are marked with one or two dots. The underlined sequences with solid line, dashed line, and dashed line with two dots indicate the [2Fe-2S] redox center I (FesSI), [2Fe-2S] redox center II (FesSII), and FAD binding domain (FAD), respectively. The box shows part of the molybdenum cofactor and substrate-binding domain (MoCo). The accession numbers of *Sus scrofa* (Ss) AOX1, *Bos taurus* (Bt) AOX1, *Homo sapiens* (Hs) AOX1, *Mus musculus* (Mm) AOX1, *Pongo abelii* (Pa) AOX1, *Oryctolagus cuniculus* (Oc) AOX1, and *Rattus norvegicus* (Rn) AOX1 are AGC31499, NP_788841, NP_001150, NP_033806, NP_001125740, NP_001075459, and NP_062236 respectively.

by 7.5% native PAGE under cool conditions and then immunoblotted with antibodies against aldehyde oxidase.

Enzyme Activity Assays Using Quinoxaline-1,4-Dioxides. The enzymatic activities were measured using three quinoxaline-1,4-dioxides: quinocetone, mequindox, and cyadox, and their derivatives: 1-deoxyquinocetone, 1-deoxy mequindox, and 1-deoxy cyadox. SsAOX1 (50 μg/ml) in a buffer containing 50 mM Tris-HCl (pH 7.4) and 1 mM EDTA was incubated with 200 mM benzaldehyde in a final volume of 1 ml at 37°C under anaerobic conditions (99.999% N^2) for 5 minutes. Then, 2–60 μM QdNOs was added into the mixtures and maintained under anaerobic conditions (99.999% N^2) at 37°C for 60 minutes. The reactions were stopped by boiling for 10 minutes followed by adding 3 ml ethyl acetate, vortexing, and centrifuging at 500*g* for 10 minutes. The supernatants were then dried under N^2, redissolved in 200 μl methanol, and subjected to HPLC for analysis. HPLC was performed using a Waters 2695 HPLC System equipped with a Waters 2487 Dual λ absorbance detector. To separate QdNOs and the reduced metabolites, 20 μl of the samples were injected into an Agilent TC18 (2) column (250 mm × 4.6 mm, 5μm). The mobile phase consisted of solvent A (0.1% formic acid) and solvent B (methanol). The gradient elution program was set as follows: 0–5 minutes, 15% solvent B; 5–25 minutes, 15% to 60% solvent B; 25–25.1 minutes, 60% to 100% solvent B; 25.1–30 minutes, 15% solvent B. The wavelength was set at 305 nm. The quantitative analyses of N1-deoxyquinocetone, N1-deoxy mequindox, and N1-deoxycyadox were performed according to the peak area. Kinetic parameters for the biotransformation of N1-deoxyquinocetone, N1-deoxy mequindox, and N1-deoxycyadox were calculated by fitting data into the Michaelis-Menten equation, $v = V_{max}[S] / (K_m + [S])$ by GraphPad Prism 5 software.

Site-directed Mutagenesis and Enzyme Activity Assay. *SsAOX1* cDNA in the pQE-30 expression vector was mutagenized using the QuikChange II site-directed mutagenesis kit (Stratagene, Santa Clara, CA). The mutagenesis was performed according to the manufacturer's suggested protocol. Primers were designed using the online tool provided by Stratagene and listed in Supplemental Table 2. All mutations were verified by sequencing (Invitrogen, Guangzhou, China).

After expression, all of the mutants were tested for activity toward benzaldehyde by the method of Enrico Garattini (Schumann et al., 2009). Briefly, the enzyme assays were performed at 30°C in Tris buffer (50 mM, 1 mM EDTA, pH 7.4) in a final volume of 0.5 ml. The total enzyme concentration was 30 nM for wild-type SsAOX1 or variants. The enzyme activity was spectrophotometrically monitored at 600 nm with 100 mM 2,6-dichlorphenolindophenol as the electron acceptor. The activity of SsAOX1 G1019T toward the QdNOs was evaluated as described above.

Results

cDNA Cloning of Aldehyde Oxidase from Pig Livers. Through reverse-transcription PCR using degenerate primers based on the sequence similarity of mammalian *AOX1*, three PCR products were obtained and assembled to produce the full-length porcine *AOX1* (data not shown). The cloned porcine *AOX1* was named *SsAOX1* (GenBank accession No. JX977168). The open reading frame of *SsAOX1* is 4017 bp, which encodes a 1338-residue polypeptide. The deduced protein has a molecular mass of 147,710 Da and exhibited an 87% amino acid sequence identity with human and bovine AOX1 (data not shown). Genomic analysis showed that *SsAOX1* is located on chromosome 15 in the genome of *Sus scrofa* and bears 35 exons and 34 introns (Fig. 2A).

Motif prediction and amino acid sequence alignment showed that SsAOX1 is a typical aldehyde oxidase, containing two nonidentical 2Fe-2S centers in the N terminus, an FAD-binding region in the intermediate region, and a molybdenum cofactor and substrate pocket in the C terminus (Fig. 2A). The alignment of SsAOX1 with other mammalian AOX1 showed that these motifs are very conserved among mammalian AOX1 (Fig. 2B).

Recombinant Expression and Characterization of SsAOX1 in *E. coli*. A His-tagged SsAOX1 protein of approximately 150 kDa was expressed (Fig. 3). Similar to other reported AOs (Kurosaki et al., 2004), a major band with a molecular mass of 150 kDa and two minor degraded bands of approximately 130 and 80 kDa were detected by

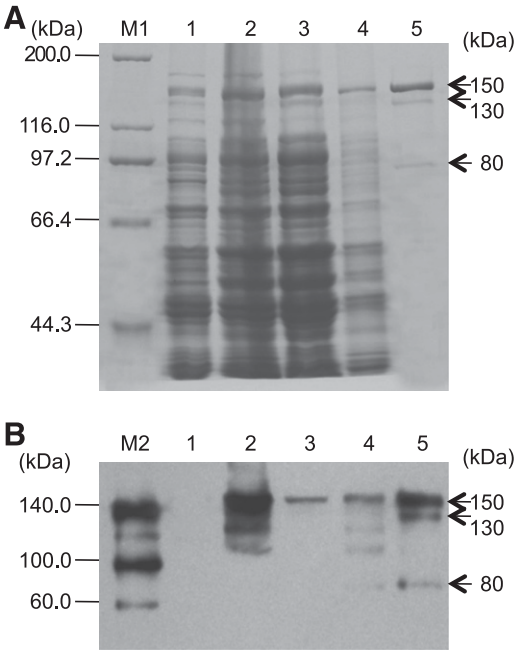

Fig. 3. Recombinant expression and purification of SsAOX1 in *E. coli*. (A) SDS-PAGE analysis of the expression of SsAOX1in *E. coli* M15. M1 indicates the SDS-PAGE protein standards. Lanes 1–5 indicate the noninduced cells, IPTG-induced cells, the soluble cell extracts, cell debris, and purified SsAOX1, respectively. (B) Western blot analysis of the expression and purification of SsAOX1. M2 indicates the biotin-labeled protein standards. Lanes 1–5 indicate the same sample as A.

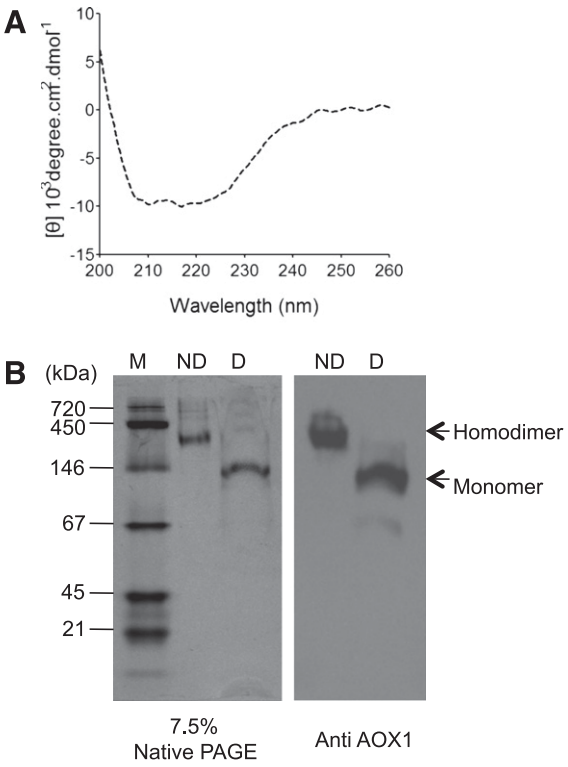

Fig. 4. Structure characterization of SsAOX1. (A) The circular dichroism spectra of SsAOX1. (B) Analysis of SsAOX1 on native PAGE. D, SsAOX1in denatured buffer and boiled at 100°C for 10 minutes; M, native protein molecular standards; ND, SsAOX1in native buffer.

SDS-PAGE (Fig. 3A) and confirmed by Western blot analysis using an antibody against AOX1 (Santa Cruz Biotechnology) (Fig. 3B).

Circular dichroism (CD) is a useful technique for the structural study of proteins. We investigated the secondary structures of SsAOX1 by CD. As shown in Fig. 4A, the CD spectra of SsAOX1 exhibited the characteristic signature of an α helix, with minima at 222 and 208 nm. The spectrum corresponds to the SsAOX1 protein with secondary structures of 32.7% α-helix, 17.6% β-sheet, 16.9% β-turn, and approximately 54% other.

Because AO was reported to function as a homodimer, the native formation of SsAOX1 was analyzed by native PAGE. As shown in Fig. 4B, the SsAOX1 in native sample buffer ran at approximately 300 kDa, whereas the boiled SsAOX1 in denaturation buffer ran at approximately 150 kDa, which indicates the purified SsAOX1 formed a functional homodimer under native conditions.

SsAOX1 Catalyzed *N*-Oxide Reduction of Quinoxaline 1,4-di-*N*-Oxides at the N1 Position. To determine whether the recombinant expressed and purified SsAOX1 could catalyze the *N*-oxide reduction of QdNOs, three representative QdNOs: quinocetone, mequindox, and cyadox (Fig. 1), were incubated with SsAOX1, and the metabolites were detected by HPLC. After the reaction, only the N1-deoxidized products of the three tested drugs were clearly detected, whereas no N4-deoxidized products were detected (Fig. 5; Supplemental Fig. 4). Furthermore, the N1-deoxidization was inhibited by an AO inhibitor (chlorpromazine) and abolished by boiling the proteins (data not shown), indicating that the N1-deoxidization was catalyzed by AO, and the N-O bond at N1 position might be more resistant than that of N4 position to reduction by AO. Subsequently, the enzyme kinetic parameters were determined. The results showed that SsAOX1 had a highest activity to quinocetone, followed by mequindox and cyadox, with the *k*cat/K_m values of 1.94 ± 0.04, 1.27 ± 0.15, and 0.43 ± 0.09 minute^{-1} μM^{-1}, respectively (Table 1). However, SsAOX1 had lowest substrate affinity to quinocetone, followed by cyadox and mequindox, with K_m values of 4.36 ± 0.56, 3.16 ± 0.48, and 2.96 ± 0.51 μM, respectively (Table 1).

Substitution of Glycine 1019 with Threonine Endows SsAOX1 with *N*-Oxide Reductive Activity at the N4 Position of Quinoxaline 1,4-di-*N*-Oxides. To further elucidate the catalytic mechanism of SsAOX1 toward the QdNOs, five mutants at amino acid 1019, which is one of the active sites in substrate binding pocket (Dastmalchi, 2005), were generated and analyzed. Because the reduction of AO by the oxidation of its substrate (e.g., benzaldehyde and 4,6-dihydroxypyrimidine) is a vital step for the subsequent reduction of the N-O bond (Sugihara et al., 1996), the activity of mutants toward its standard substrate, benzaldehyde, was analyzed. The G1019T mutant exhibited a 6-fold increase in benzaldehyde oxidation activity, whereas the other four mutants displayed a negligible effect (Table 2). Therefore, the activity of the G1019T mutant toward the QdNOs was further analyzed. Interestingly, the N1, N4 double deoxidized metabolites were detected with all of the three tested QdNOs drugs, whereas no detectable single N4 deoxidized metabolites were detected (Fig. 6; Supplemental Fig. 5).

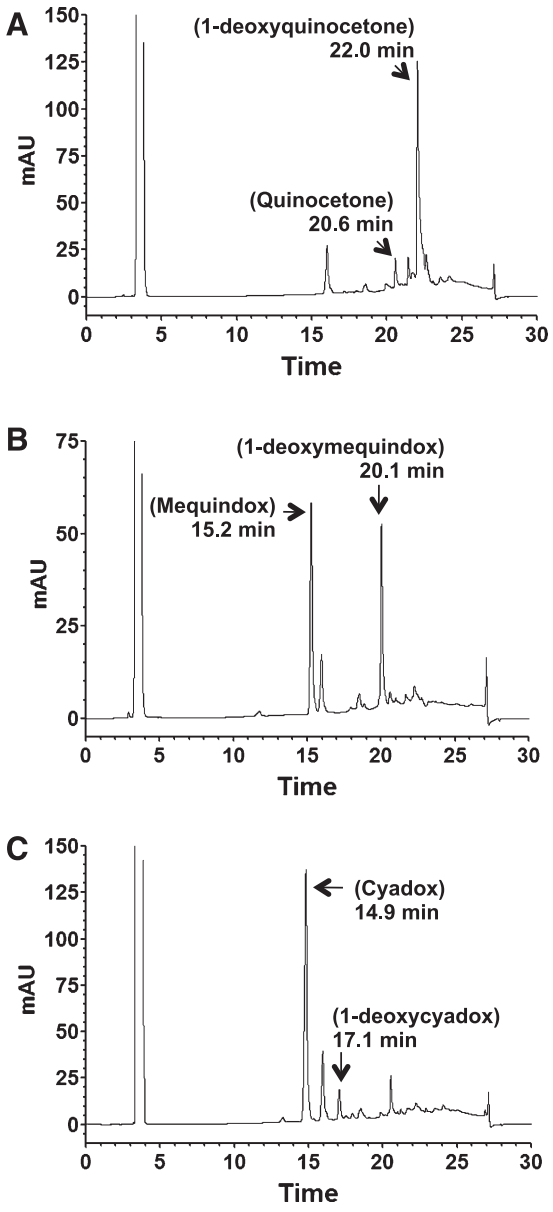

Fig. 5. The HPLC chromatographs of SsAOX1-metabolized quinocetone, mequindox, and cyadox. The arrows indicate the peaks of quinocetone, mequindox, cyadox, and their *N*-oxide-reduced metabolites. Quinocetone, 1-deoxyquinocetone, 4-deoxyquinocetone, and 1,4-dideoxyquinocetone were eluted at 20.6, 22.0, 21.3, and 22.6 minutes, respectively. Mequindox, 1-deoxymequindox, 4-deoxymequindox, and 1,4-dideoxymequindox were eluted at 15.2, 20.1, 17.9, and 21.2 minutes, respectively. Cyadox, 1-deoxycyadox, 4-deoxycyadox, and 1,4-dideoxycyadox were eluted at 14.9, 17.1, 17.9, and 18.7 minutes, respectively.

To further confirm the N4-deoxidizing activity of mutant G1019T, the N1-deoxidized metabolites of the QdNOs (1-deoxyquinocetone, 1-deoxymequindox, and 1-deoxycyadox) were incubated with SsAOX1

TABLE 1

Enzymatic kinetic parameters of SsAOX1 toward quinocetone, mequindox, and cyadox

The values represent the mean ± S.D. of three experiments.

Kinetic Parameters	Quinocetone	Mequindox	Cyadox
V_{max} [nmol/min·mg protein]	2882.52 ± 11.32	1276.45 ± 62.13	463.5 ± 20.0
K_m [μM]	4.36 ± 0.56	2.96 ± 0.51	3.16 ± 0.48
k_{cat} [min^{-1}][a]	8.47 ± 0.03	3.75 ± 0.16	1.36 ± 0.06
k_{cat}/K_m [min^{-1}μM^{-1}]	1.94 ± 0.04	1.27 ± 0.15	0.43 ± 0.09

[a]k_{cat} was calculated from Mr 147,000

TABLE 2

Enzymatic kinetic parameters of SsAOX1 and variants toward benzaldehyde

The values represent the mean ± S.D. of three experiments.

Protein	Kinetic Parameters for Benzaldehyde[a]			
	V_{max}	K_m	k_{cat}	k_{cat}/K_m
	nmol/min·mg protein	*μM*	min^{-1}	$min^{-1}\mu M^{-1}$
Wild-Type	19380 ± 1750.50	8.76 ± 1.21	646.62 ± 58.35	73.74 ± 1.96
G1019T	24270 ± 2283.65	1.90 ± 0.233	809.37 ± 76.12	426.73 ± 6.74
G1019A	22290 ± 2497.53	6.42 ± 0.759	743.52 ± 83.25	115.82 ± 4.59
G1019D	9120 ± 1194.26	10.60 ± 2.04	304.34 ± 39.83	30.62 ± 8.47
G1019E	11160 ± 1357.81	15.73 ± 3.97	372 ± 45.26	24.25 ± 1.92
G1019K	10230 ± 950.15	13.80 ± 2.64	341 ± 31.67	24.73 ± 1.73

[a] k_{cat} was calculated from Mr 147,000.

G1019T and compared with wild-type SsAOX1 in the same reaction system. After the reaction, obvious N1, N4 double deoxidized metabolites were detected in the reaction with mutant G1019T (Fig. 7, A–C), whereas no or small amount of N1, N4 double deoxidized metabolites were detected with wild-type SsAOX1 (Fig. 7, D–F), indicating that G1019T endowed SsAOX1 with the N4 deoxidizing activity toward the QdNOs. However, it is not clear whether the N-4 reduction requires the N-1 reduction or not. It is possible SsAOX1 G1019T can reduce N4 before N1 reduction, but the reduction of N1 occurs more readily than that of N4 (Shen et al., 2010, 2012; Zheng et al., 2011) (Fig. 5). Therefore, the 4-deoxy products generated by SsAOX1 G1019T may not be easy to detect.

Discussion

The QdNOs consist of a group of quinoxaline derivatives, which are widely used as human drugs and animal feed additives. However, the genotoxicity and reproductive toxicity of QdNOs has been reported recently (Ihsan et al., 2011, 2013). The *N*-oxide groups of QdNOs are the main functional moiety responsible for their activity and toxicity (Carta et al., 2005). Thus, understanding the metabolic mechanism of the *N*-oxide groups is important for the application and administration of QdNOs. In this study, the *N*-oxide reduction enzyme for QdNOs in swine, SsAOX1, was identified and characterized. SsAOX1 catalyzed the *N*-oxide reduction at the N1 position, and the substitution of glycine 1019 with threonine endows the enzyme with the *N*-oxide reductive activity at the N4 position.

AOs are capable of transforming a wide array of substrates. Along with the presence of significant levels of enzymatic activity in the cytosolic fraction, AOs have attracted increasing interest in the drug metabolism and drug discovery fields (Garattini et al., 2008; Pryde et al., 2010; Garattini and Terao, 2011, 2013). AOs can function not only as oxidases but also as reductases. The oxidizing substrate varies from aldehyde-containing compounds to various types of aromatic azo-and oxo-heterocyclic compounds and iminium-containing compounds (Garattini and Terao, 2011, 2012). The reduction substrates include *N*-oxides, sulfoxides, nitro-compounds, and heterocycles (Tatsumi et al., 1982, 1983; Kitamura and Tatsumi, 1984). In this study, we cloned and characterized the AO isoform in swine for *N*-oxide reduction of three widely used QdNOs (quinocetone, mequindox, and cyadox) in animal feed additives. The N-O bonds were shown to be not only the activity group of the QdNOs but also the toxicity group (Carta et al., 2005). Hence, understanding the metabolic pathways of *N*-oxide reduction of the QdNOs is important for their application and administration. Previously, we have shown that cyadox could be metabolized to 1-deoxycyadox and 4-deoxycyadox in pig liver extracts (Zheng et al., 2011). Using the inhibitor approach, we showed that the metabolism might be catalyzed by AO and XO (Zheng et al., 2011). However, SsAOX1 could only metabolize cyadox to 1-deoxycyadox (Fig. 5C). Because the number of AOs can range from one to four in vertebrates (Garattini et al., 2009;

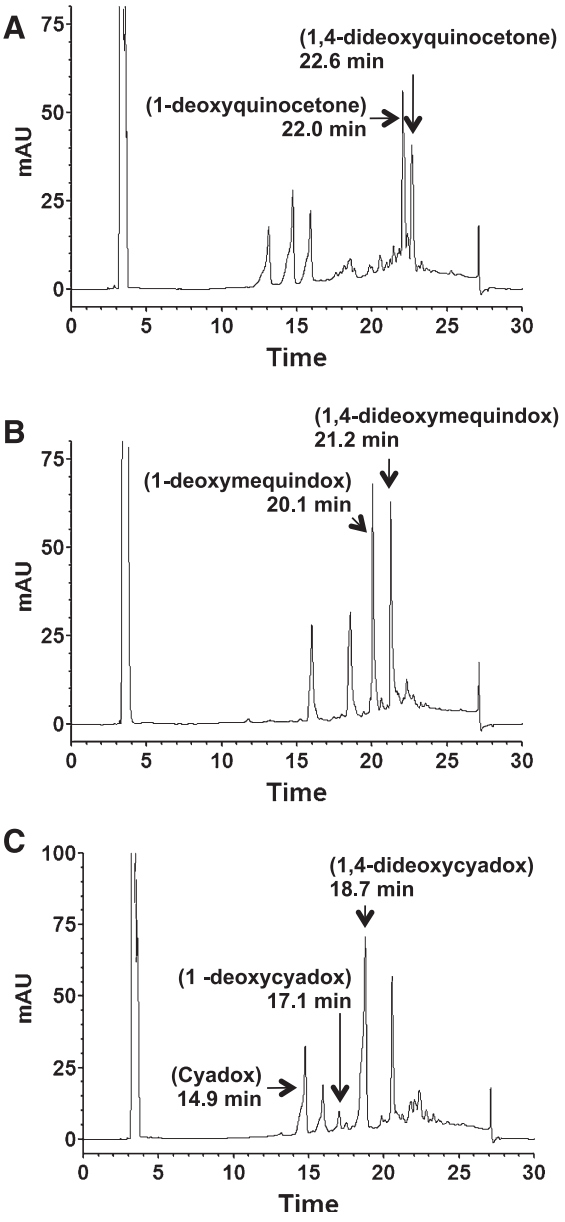

Fig. 6. The HPLC chromatographs of SsAOX1 G1019T-metabolized quinocetone (A), mequindox (B), and cyadox (C). The arrows indicate the peaks of quinocetone, mequindox, cyadox, and their *N*-oxide-reduced metabolites.

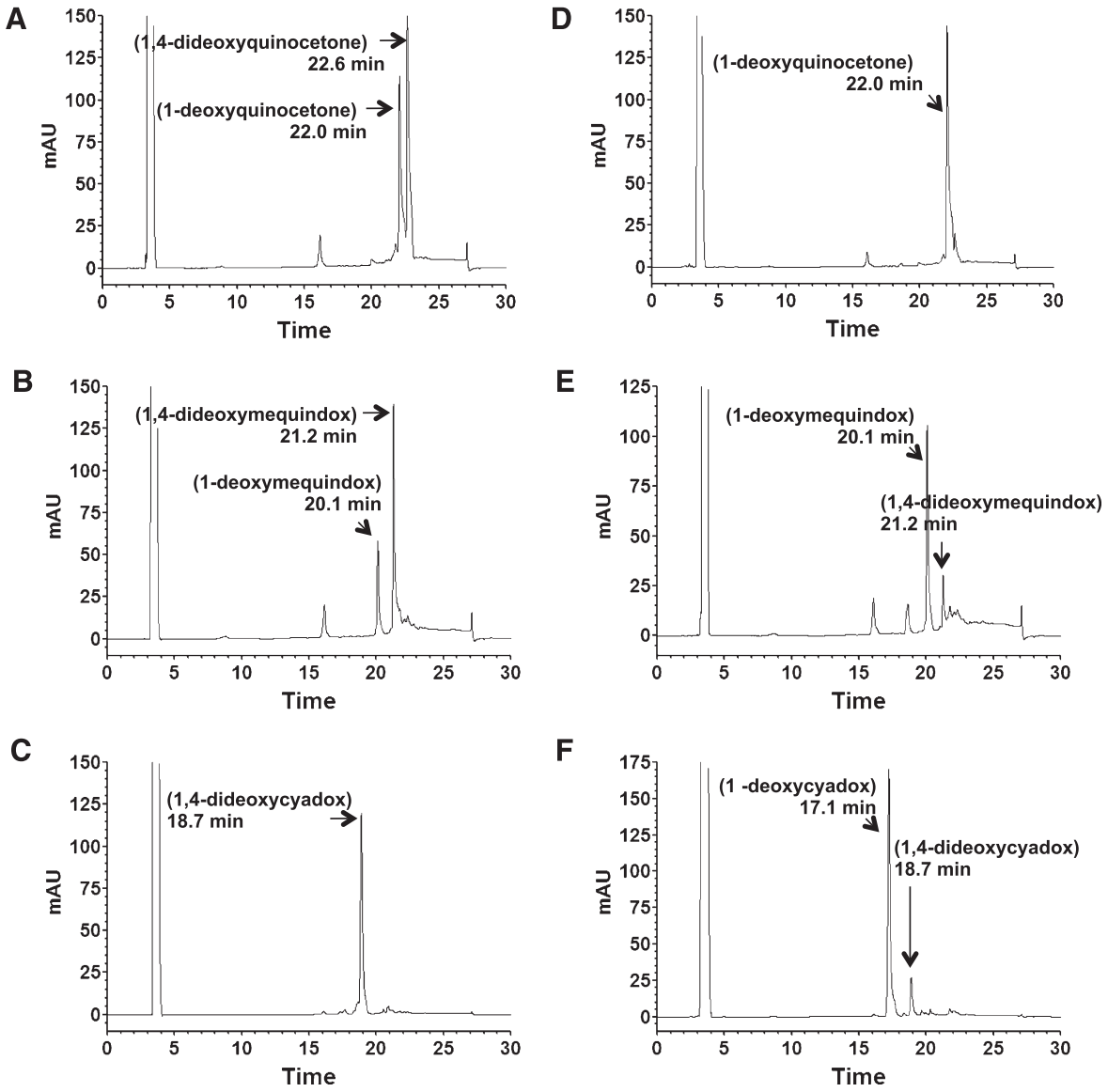

Fig. 7. The HPLC chromatographs of SsAOX1 or SsAOX1 G1019T–metabolized N1-reduced QdNOs. (A) SsAOX1 G1019T–metabolized 1-deoxyquinocetone. (B) SsAOX1-metabolized G1019T 1-deoxymequindox. (C) SsAOX1 G1019T–metabolized 1-deoxycyadox. (D) SsAOX1-metabolized 1-deoxyquinocetone. (E) SsAOX1-metabolized 1-deoxymequindox. (F) SsAOX1-metabolized 1-deoxycyadox. The arrows indicate the peaks of quinocetone, mequindox, cyadox, and their *N*-oxide reduced-metabolites.

Kurosaki et al., 2013), we propose that there is another AO or XO responsible for the *N*-oxide reduction at the N4 position of the QdNOs quinocetone, mequindox, and cyadox.

Interestingly, SsAOX1 primarily catalyzed the *N*-oxide reduction at the N1 position of the three tested QdNOs (Fig. 5). This result is in agreement with the metabolism profile of quinocetone and mequindox. Shen et al. showed that 1-deoxyquinocetone was abundant in swine urine, but 4-deoxyquinocetoone was not (Shen et al., 2010). Shan et al. (2012) showed that 1-deoxymequindox was more abundant than 4-deoxymequindox in chicken. We propose that the high abundance of the N1-reduced metabolites may be partially due to the activity of AO and the structure of these drugs. It was reported that N1 reduction can happen either by enzymatic or nonenzymatic catalysis (Zheng et al., 2011), but the same is not true for N4 reduction, which indicates that the N-O bond at the N1 position is not as stable as the N4 position. The difference between the N-O bonds at the N1 position and the N4 position is that the N-O bond at the N1 position is closer to the electron-withdrawing group at the C2 position (Fig. 1). Based on the structure of three QdNOs and the in vivo and in vitro metabolism data, we propose that the electron groups adjacent to the N-O bond may influence its stability. Therefore, it would be helpful to clarify this by changing the group at the C-2 and C-3 positions. Several researchers have attempted to modify the molecular structure of drugs to prevent them from being metabolized by AO (Linton et al., 2011; Pryde et al., 2012). For *N*-oxide reduction, our results may contribute to this approach, with our suggestion of modification of the groups adjacent to the N-O bond. However, through site-directed mutagenesis, we found that the substitution of glycine 1019 with threonine at the substrate-binding pocket endows SsAOX1 with *N*-oxide reductive activity at N4 position of the QdNOs (Figs. 6 and 7, A–C). There is a hydroxyl group at the side chain of threonine, whereas glycine does not contain that group. The amino acid at 1019 was reported to be one of the most important active sites, which is located in close proximity to the substrate (Enroth et al., 2000; Dastmalchi, 2005; Coelho et al.,

2012). Because threonine has a nucleophilic side chain, whereas glycine has not, we hypothesize that the nucleophilic side chain of the amino acid at 1019 may increase the interaction between AO and N-O bonds.

In conclusion, this study identified the enzyme (SsAOX1) for *N*-oxide reduction of QdNOs in swine. SsAOX1 catalyzed the *N*-oxide reduction at the N1 position of the QdNOs, and its activity might be influenced by the composition of the C2 group of its substrate. Furthermore, the substitution of glycine 1019 with threonine endows SsAOX1 with *N*-oxide reductive activity at the N4 position of the QdNOs. However, the mechanism of *N*-oxide reduction of QdNOs is not yet entirely clear. To better understand it, the substitution of groups at the C2 and C3 positions would be helpful and might spark interest in further research.

Authorship Contributions

Participated in research design: Deng, Mu, M. Zheng.

Conducted experiments: Mu, Tang, Y. Wang, Wu, Xu, M. Zheng, Y. Zheng.

Performed data analysis: Chen, Deng, Mu, L. Wang, M. Zheng.

Wrote or contributed to the writing of the manuscript: Deng, Mu, M. Zheng.

References

Beedham C (1987) Molybdenum hydroxylases: biological distribution and substrate-inhibitor specificity. *Prog Med Chem* **24**:85–127.

Beutin L, Preller E, and Kowalski B (1981) Mutagenicity of quindoxin, its metabolites, and two substituted quinoxaline-di-N-oxides. *Antimicrob Agents Chemother* **20**:336–343.

Bickel MH (1969) The pharmacology and biochemistry of N-oxides. *Pharmacol Rev* **21**: 325–355.

Carta A, Corona P, and Loriga M (2005) Quinoxaline 1,4-dioxide: a versatile scaffold endowed with manifold activities. *Curr Med Chem* **12**:2259–2272.

Coelho C, Mahro M, Trincão J, Carvalho AT, Ramos MJ, Terao M, Garattini E, Leimkühler S, and Romão MJ (2012) The first mammalian aldehyde oxidase crystal structure: insights into substrate specificity. *J Biol Chem* **287**:40690–40702.

Dastmalchi S, Hamzeh-Mivehrod M (2005) Molecular modelling of human aldehyde oxidase and identification of the key interactions in the enzyme-substrate complex. *DARU J Pharm Sci* **13**: 82–93.

Enroth C, Eger BT, Okamoto K, Nishino T, Nishino T, and Pai EF (2000) Crystal structures of bovine milk xanthine dehydrogenase and xanthine oxidase: structure-based mechanism of conversion. *Proc Natl Acad Sci USA* **97**:10723–10728.

Garattini E, Fratelli M, and Terao M (2008) Mammalian aldehyde oxidases: genetics, evolution and biochemistry. *Cell Mol Life Sci* **65**:1019–1048.

Garattini E, Fratelli M, and Terao M (2009) The mammalian aldehyde oxidase gene family. *Hum Genomics* **4**:119–130.

Garattini E and Terao M (2011) Increasing recognition of the importance of aldehyde oxidase in drug development and discovery. *Drug Metab Rev* **43**:374–386.

Garattini E and Terao M (2012) The role of aldehyde oxidase in drug metabolism. *Expert Opin Drug Metab Toxicol* **8**:487–503.

Garattini E and Terao M (2013) Aldehyde oxidase and its importance in novel drug discovery: present and future challenges. *Expert Opin Drug Discov* **8**:641–654.

Hille R (1996) The Mononuclear Molybdenum Enzymes. *Chem Rev* **96**:2757–2816.

Hille R (2002) Molybdenum and tungsten in biology. *Trends Biochem Sci* **27**:360–367.

Hille R (2005) Molybdenum-containing hydroxylases. *Arch Biochem Biophys* **433**:107–116.

Huang XJ, Zhang HH, Wang X, Huang LL, Zhang LY, Yan CX, Liu Y, and Yuan ZH (2010) ROS mediated cytotoxicity of porcine adrenocortical cells induced by QdNOs derivatives in vitro. *Chem Biol Interact* **185**:227–234.

Ihsan A, Wang X, Liu Z, Wang Y, Huang X, Liu Y, Yu H, Zhang H, Li T, and Yang C, et al. (2011) Long-term mequindox treatment induced endocrine and reproductive toxicity via oxidative stress in male Wistar rats. *Toxicol Appl Pharmacol* **252**:281–288.

Ihsan A, Wang X, Zhang W, Tu H, Wang Y, Huang L, Iqbal Z, Cheng G, Pan Y, and Liu Z, et al. (2013) Genotoxicity of quinocetone, cyadox and olaquindox in vitro and in vivo. *Food Chem Toxicol* **59**:207–214.

Kitamura S, Sugihara K, and Tatsumi K (1999) A unique tertiary amine N-oxide reduction system composed of quinone reductase and heme in rat liver preparations. *Drug Metab Dispos* **27**:92–97.

Kitamura S and Tatsumi K (1984) Involvement of liver aldehyde oxidase in the reduction of nicotinamide N-oxide. *Biochem Biophys Res Commun* **120**:602–606.

Kurosaki M, Bolis M, Fratelli M, Barzago MM, Pattini L, Perretta G, Terao M, and Garattini E (2013) Structure and evolution of vertebrate aldehyde oxidases: from gene duplication to gene suppression. *Cell Mol Life Sci* **70**:1807–1830.

Kurosaki M, Terao M, Barzago MM, Bastone A, Bernardinello D, Salmona M, and Garattini E (2004) The aldehyde oxidase gene cluster in mice and rats. Aldehyde oxidase homologue 3, a novel member of the molybdo-flavoenzyme family with selective expression in the olfactory mucosa. *J Biol Chem* **279**:50482–50498.

Linton A, Kang P, Ornelas M, Kephart S, Hu Q, Pairish M, Jiang Y, and Guo C (2011) Systematic structure modifications of imidazo[1,2-a]pyrimidine to reduce metabolism mediated by aldehyde oxidase (AO). *J Med Chem* **54**:7705–7712.

Liu ZY, Huang LL, Chen DM, Dai MH, Tao YF, and Yuan ZH (2010a) The metabolism and N-oxide reduction of olaquindox in liver preparations of rats, pigs and chicken. *Toxicol Lett* **195**:51–59.

Liu ZY, Huang LL, Chen DM, and Yuan ZH (2010b) Metabolism of mequindox in liver microsomes of rats, chicken and pigs. *Rapid Commun Mass Spectrom* **24**:909–918.

Liu ZY and Sun ZL (2013) The metabolism of carbadox, olaquindox, mequindox, quinocetone and cyadox: an overview. *Med Chem* **9**:1017–1027 Epub ahead of print.

Ortega MA, Montoya ME, Jaso A, Zarranz B, Tirapu I, Aldana I, and Monge A (2001) Antimycobacterial activity of new quinoxaline-2-carbonitrile and quinoxaline-2-carbonitrile 1,4-di-N-oxide derivatives. *Pharmazie* **56**:205–207.

Pryde DC, Dalvie D, Hu Q, Jones P, Obach RS, and Tran TD (2010) Aldehyde oxidase: an enzyme of emerging importance in drug discovery. *J Med Chem* **53**:8441–8460.

Pryde DC, Tran TD, Jones P, Duckworth J, Howard M, Gardner I, Hyland R, Webster R, Wenham T, and Bagal S, et al. (2012) Medicinal chemistry approaches to avoid aldehyde oxidase metabolism. *Bioorg Med Chem Lett* **22**:2856–2860.

Schumann S, Terao M, Garattini E, Saggu M, Lendzian F, Hildebrandt P, and Leimkühler S (2009) Site directed mutagenesis of amino acid residues at the active site of mouse aldehyde oxidase AOX1. *PLoS ONE* **4**:e5348.

Shan Q, Liu Y, He L, Ding H, Huang X, Yang F, Li Y, and Zeng Z (2012) Metabolism of mequindox and its metabolites identification in chickens using LC-LTQ-Orbitrap mass spectrometry. *J Chromatogr B Analyt Technol Biomed Life Sci* **881-882**:96–106.

Shen J, Yang C, Wu C, Feng P, Wang Z, Li Y, Li Y, and Zhang S (2010) Identification of the major metabolites of quinocetone in swine urine using ultra-performance liquid chromatography/electrospray ionization quadrupole time-of-flight tandem mass spectrometry. *Rapid Commun Mass Spectrom* **24**:375–383.

Sugihara K, Kitamura S, and Tatsumi K (1996) S-(-)-nicotine-1′-N-oxide reductase activity of rat liver aldehyde oxidase. *Biochem Mol Biol Int* **40**:535–541.

Suter W, Rosselet A, and Knüsel F (1978) Mode of action of quindoxin and substituted quinoxaline-di-N-oxides on Escherichia coli. *Antimicrob Agents Chemother* **13**:770–783.

Takekawa K, Sugihara K, Kitamura S, and Ohta S (2001) Enzymatic and non-enzymatic reduction of brucine N-oxide by aldehyde oxidase and catalase. *Xenobiotica* **31**:769–782.

Takekawa K, Sugihara K, Kitamura S, and Tatsumi K (1997) Nonenzymatic reduction of brucine N-oxide by the heme group of cytochrome P450. *Biochem Mol Biol Int* **42**:977–981.

Tatsumi K, Kitamura S, and Yamada H (1982) Involvement of liver aldehyde oxidase in sulfoxide reduction. *Chem Pharm Bull (Tokyo)* **30**:4585–4588.

Tatsumi K, Yamada H, and Kitamura S (1983) Evidence for involvement of liver aldehyde oxidase in reduction of nitrosamines to the corresponding hydrazine. *Chem Pharm Bull (Tokyo)* **31**:764–767.

Vicente E, Villar R, Pérez-Silanes S, Aldana I, Goldman RC, and Mong A (2011) Quinoxaline 1,4-di-N-oxide and the potential for treating tuberculosis. *Infect Disord Drug Targets* **11**:196–204.

Wu H, Yang C, Wang Z, Shen J, Zhang S, Feng P, Li L, and Cheng L (2012) Metabolism profile of quinocetone in swine by ultra-performance liquid chromatography quadrupole time-of-flight mass spectrometry. *Eur J Drug Metab Pharmacokinet* **37**:141–154.

Zheng M, Jiang J, Wang J, Tang X, Ouyang M, and Deng Y (2011) The mechanism of enzymatic and non-enzymatic N-oxide reductive metabolism of cyadox in pig liver. *Xenobiotica* **41**:964–971.

Address correspondence to: Yiqun Deng, College of Life Sciences, South China Agricultural University, No. 483, Wushan Road, Guangzhou, Guangdong 510642, China. E-mail: yqdeng@scau.edu.cn